

BEAN-SHAPED ADVANCED STELLARATORS WITH MODULAR COIL SYSTEMS

F. Herrnegger and F. Rau

*Max-Planck-Institut für Plasmaphysik
IPP-EURATOM Association
D-8046 Garching bei München*

Abstract

Bean-shaped Advanced Stellarator configurations with a nearly plane magnetic axis, small shear, an aspect ratio of $A = 10 - 12$, and $m = 5$ field periods around the torus are investigated. These configurations are given by Dommaschk potentials. Associated modular coil systems with a coil aspect ratio of about 5.5 and 18 to 6 coils per field period are derived. For such vacuum field configurations with a magnetic well, values of $\langle j_{\parallel}/j_{\perp} \rangle = 0.8$ to 2.2 are obtained at $\epsilon = 0.48$ to 0.31. By comparison, the corresponding values of W VII-AS are $\langle j_{\parallel}/j_{\perp} \rangle = 2.2$ to 1.9 at $\epsilon = 0.39$.

1. Introduction

Advanced Stellarator configurations ¹⁾ with an average magnetic well are characterized by a reduced drift of particles away from a magnetic surface, reduced secondary currents, and thus by a reduced Shafranov shift of the magnetic surfaces compared with a classical stellarator. Configurations like the Advanced Stellarator Wendelstein W VII - AS ²⁾ are shown by numerical computation to allow an average value for the equilibrium- β of up to approximately $\langle \beta \rangle \approx 5\%$ ³⁾, whereas calculations of the stability- β yield considerably lower values. On the other hand, spatial axis configurations like Helias ⁴⁾ afford prospects of stability- β values of up to 5%.

In the present paper, Bean-shaped Advanced Stellarators with a nearly plane magnetic axis and associated modular coil systems are introduced where the magnetic field is represented by Dommaschk ⁵⁾ potentials. Modular coil systems are derived from these potentials. Typical parameter values are $m = 5$ field periods, aspect ratio of the last closed magnetic surface $A = R_T/a = m L_P/2\pi a \approx 10$ to 12 (a is the average minor radius of the last closed magnetic surface and R_T the major torus radius), a magnetic well of the vacuum field $(V' - V'_0)/V'_0$ down to -2.5% , twist (rotational transform) at the magnetic axis around $t_0 = 0.4$, and small shear.

2. Configuration Studies

We consider three different examples of Bean-shaped Advanced Stellarator configurations (see Fig.1), which are characterized by a certain indentation of the vertically elongated magnetic surfaces at the beginning of a field period (FP). The dependence of the twist $\epsilon(r)$ and the specific volume $V' = \oint d\ell/B$ (normalized to its value on the magnetic axis) on the average minor radius r of the magnetic surfaces is shown in Figs.2 and 3. Configurations with labels FZH are given in Dommaschk potentials, those with FFR are from a system of 9 twisted coils per FP. For comparison, the standard case of W VII-AS is entered, too. All configurations have a magnetic well ($V'' < 0$).

As a figure of merit in comparing the different configurations we use the average ratio $\langle j_{\parallel}/j_{\perp} \rangle$ and the quantity $J^* = \langle (B_0^2/B^2)[1 + (j_{\parallel}/j_{\perp})^2] \rangle$, where B_0 is the reference magnetic field at R_T and $\langle \dots \rangle$ denotes the average on a magnetic surface. J^* is a measure of the Pfirsch-Schlüter currents and also appears in the stability criterion of resistive interchange modes. The ratio $\langle j_{\parallel}/j_{\perp} \rangle$ is obtained from the poloidal variation of $\int dl/B$ taken along a field line over one field period. The quantities j_{\parallel} and j_{\perp} are the absolute values of the secondary and the diamagnetic current densities, respectively, which scales

as $2/\epsilon$ for a standard stellarator like W VII-A and are reduced by a factor of about 2 in the Advanced Stellarator device W VII-AS.

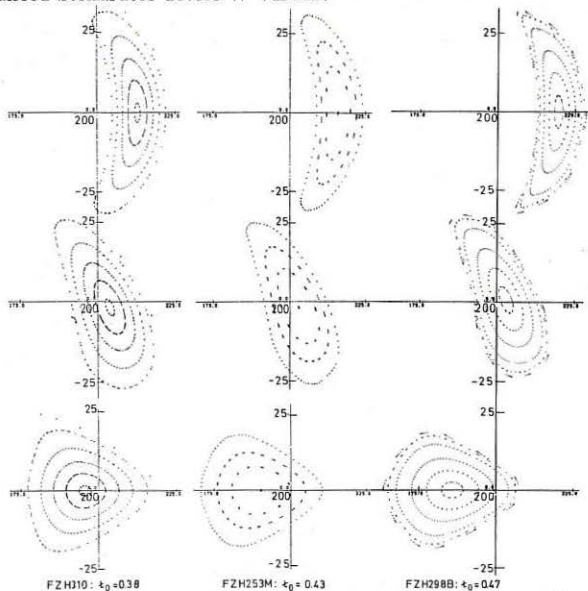


Fig.1 Cross-sections of the magnetic surfaces at 0, $Lp/4$, $Lp/2$ of a field period ($R_T = 200$ cm).

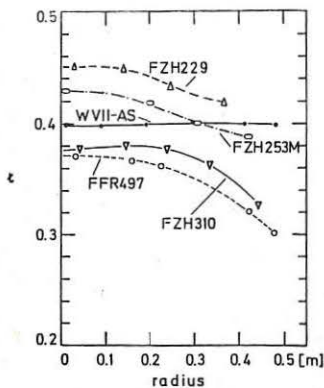


Fig.2 Twist profile.

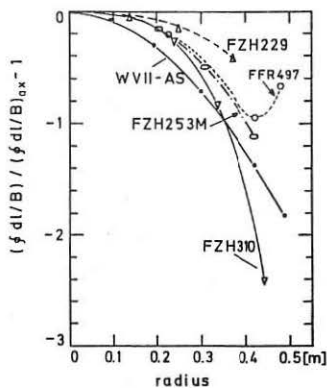


Fig.3 Specific volume.

The configuration FZH310 (see Figs.1 - 3) is characterized by a twist number at the magnetic axis $t_0 = 0.38$, a small field modulation $\delta = (B_{max} - B_{min}) / (B_{max} + B_{min}) \sim 10\%$ and a deep magnetic well of $\Delta V'/V'_0 = -2.5\%$; the reduction of the secondary currents is comparable to the W VII-AS configuration in the boundary region and is

moderately improved near the magnetic axis: $(j_{\parallel}/j_{\perp})_{ax} \approx 1.70$. The configuration FZH298B has $\epsilon_0 = 0.425$, a field modulation at the axis $\delta \sim 25\%$, and a small parallel current density of $(j_{\parallel}/j_{\perp})_{ax} \approx 0.82$. The configuration FZH253M is characterized by $\epsilon_0 = 0.43$, a moderate field ripple on axis $\delta \sim 12\%$ and $(j_{\parallel}/j_{\perp})_{ax} \approx 1.37$.

3. Modular Coil Systems

Modular systems of non-planar coils are derived for such configurations with a coil aspect ratio of around $A_c = 5.5$ and a number of coils per FP of 18, 9, or 6. For a typical number of 9 or more coils per FP the original configurations are reproduced with sufficient accuracy, whereas with 6 coils per FP a slight magnetic hill of the vacuum field is developed.

In the following example, a coil system representing the configuration FZH253M is given. As a first step, a toroidal surface with elliptical cross-section and an aspect ratio $A_c = 5.5$ is defined, where the elongation of the ellipses varies between 1.6 (at the beginning of a FP) to 1.2 (middle of a FP). The geometric centre of the cross-sections moves radially inward and outward by an amount of $\Delta R/R_T = 0.07$. On this surface 18 surface current lines⁵⁾ are computed. The discretization of this surface current distribution for a modular system of 18, 9, or 6 coils per FP is made straightforward by choosing the corresponding current lines as coil centres. At a major radius of $R_T = 500$ cm we use radial and lateral coil dimensions of 36.4 cm and 20 cm for the system with 9 coils per FP. At a gross current density of $j_{eff} = 30 \text{ MA/m}^2$ the total coil current of 2.2 MA introduces a magnetic induction of $B_{ax} = 3.7 \text{ T}$ at the magnetic axis.

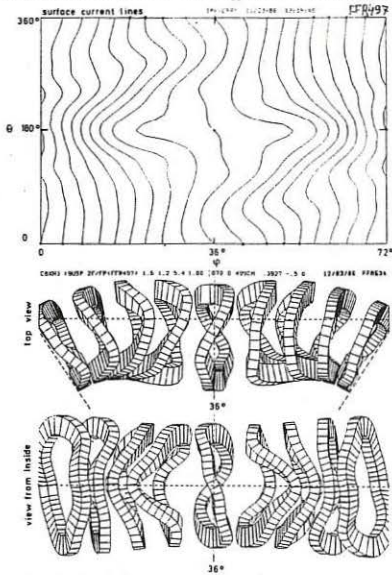


Fig.4 Angular map of surface current lines (top graph). View of coils from top (middle graph) and from inside (bottom; φ , θ are toroidal and poloidal angles).

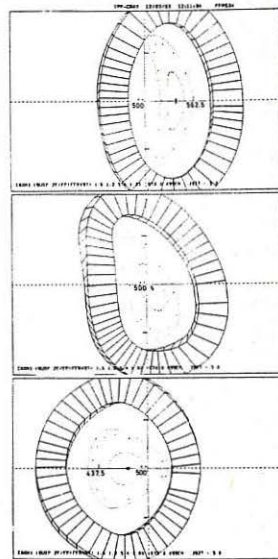


Fig.5 Cross-sections of the magnetic surfaces and shape of the adjacent coils at 0, $L_p/4$, $L_p/2$ of a field period.

The top plot of Fig. 4 shows the shape of the 18 surface current lines of one field period in an angular plot (φ, θ are the toroidal and poloidal angles); the second and third plots show the top and inside views of the modular system of the non-planar coils. There are 5 different coil shapes in the set of 9 coils per FP. The triangular cross-section of the magnetic surfaces is at $\varphi = 36^\circ$. The toroidal excursion of the coils is kept moderate by choosing an adequate aspect ratio of the surface where the surface current distribution is calculated. Configurations with other twist numbers $t_0 = 0.37 \dots 0.46$ at the magnetic axis are obtained for different values of the coil aspect ratio $A_c = 5.6 \dots 5.3$ which gives an extended parameter range compared to the original configuration FZH253M. Figure 5 shows the cross-sections of the magnetic surfaces and the shapes of the adjacent coils at toroidal positions 0, $L_P/4$, $L_P/2$ for $t_0 = 0.37$ (configuration FFR497). In comparison with W VII-AS, the coil aspect ratio is increased.

4. Summary and Conclusions

As shown in Fig. 6, the Bean-shaped Advanced Stellarators (aspect ratio $A = 10 - 12$) provide improved values of $\langle j_{\parallel}/j_{\perp} \rangle$ versus t compared to W VII-AS. For comparison, the corresponding curve for W VII-A and the relationship $2/t$ are also given. Configurations with best values $\langle j_{\parallel}/j_{\perp} \rangle_{ax} = 0.82$ and $J_{ax}^* = 1.72$ are found for $A \approx 12.4$ with a marginal magnetic well.

The BETA/BBG⁶) code is used to compute the finite- β magnetohydrostatic equilibria. An example is shown in Fig. 7 for FZH747, a data set similar to FZH298B. Preliminary finite- β computations have shown the expected reduction of the Shafranov shift accompanied by a small change of the twist profile.

The influence of the bean shape of the magnetic surfaces on the stability remains to be studied.

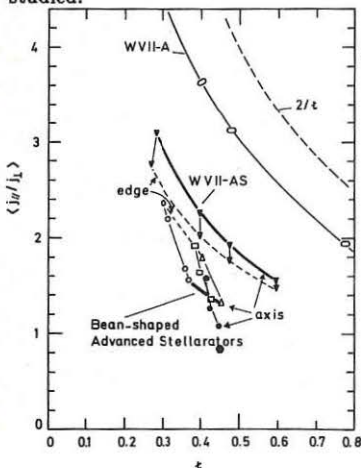


Fig. 6 Average normalized parallel current density $\langle j_{\parallel}/j_{\perp} \rangle$ as a function of twist t for various stellarators ($R_T = 200$ cm).

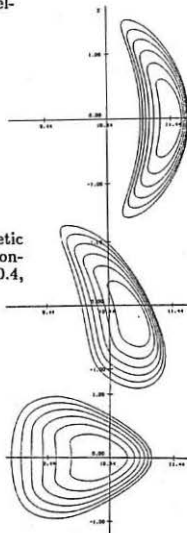


Fig. 7 Cross-sections of the magnetic surfaces at $\beta_0 = 0.07$ for configuration FZH747 ($A = 10.4$, $t_{0vac} = 0.39$).

- 1 R. Chodura, W. Dommasch, F. Herrnegger, W. Lotz, J. Nührenberg, and A. Schlüter, IEEE Trans. Plasma Science PS-9 (1981) 221.
- 2 B. Brossmann et al. Proc. 9th IAEA Conf. Baltimore, Vol. III, 141, 1982
- 3 E. Harmeyer, F. Herrnegger, J. Kißlinger, F. Rau, H. Wobig, 4th Tech. Comm. Meeting and Workshop Fusion Reactor Design and Technology (Yalta, USSR) 26 May - 6 June 1986, Paper submitted.
- 4 J. Nührenberg, R. Zille, Phys. Lett. 114A (1986) 129.
- 5 W. Dommasch, Z. Naturforsch. 37a (1982) 867.
- 6 F. Bauer, O. Betancourt, P. Garabedian, Magnetohydrodynamic Equilibrium and Stability (Springer Verlag, New York 1984).